EFFECT OF SINTERING TIME ON THE STRUCTURAL AND MAGNETIC PROPERTIES OF COBALT-CHROMIUM FERRITE NANO-PARTICLES

Y. A. Vijapure[a], S. S. More[b], U. B. Dindore[c], S. V. Rajmane[d], R. H. Kadam[e*], S. K. Akuskar[f]

[a]Chemistry Department, Shrikrishna Mahavidyalaya, Gunjoti, Tq. Omerga, Dist. Osmanabad (M.S.) India

[b]Physics Department, Y.C. College, Tuljapur, Dist. Osmanabad (M.S.) India

[c]Physics Department, Adarsh College, Omerga, Dist. Osmanabad (M.S.) India

[d]Physics Department, Jawahar College, Anadur, Tq. Tuljapur, Dist. Osmanabad (M.S.) India

[e]Physics Department, Shrikrishna Mahavidyalaya, Gunjoti, Tq. Omerga, Dist. Osmanabad (M.S.) India

[f]Chemistry Department, S.M.P. College, Murum, Tq. Omerga, Dist. Osmanabad (M.S.) India

** Corresponding author: ram111612@yahoo.co.in*

ABSTRACT

Magnetic nanoparticles of $CoCrFeO_4$ were obtained by using sol-gel auto-combustion route and sintered for two different times 4h and 8h. X-ray diffraction technique was employed to understand the crystal structure and phase formation and also to study the structural parameters influenced by changing the sintering conditions. X-ray data analysis confirms the cubic spinel structure, and the lattice parameter is observed increasing with sintering temperature. Crystallite size evaluated by using Scherrer equation is observed in nano-meter range which is confirmed by using scanning electron micrographs. Infrared spectra recorded in the range 300 cm^{-1} to 800 cm^{-1} shows two major absorption bands (ν_1) and (ν_2) which are related to ferrites with spinel structure. Increase in sintering temperature enhances the saturation magnetization (M_s), remnant magnetization (M_R) and decreases the coercive field (H_c). Sintering conditions greatly affects the structural and magnetic parameters of the ferrites with spinel structure. Hence in the present study we have reported the influence of sintering time on the properties of Co-Cr-Fe-O ferrite nanoparticles prepared by sol-gel technique.

Keywords: *Sintering time, crystallite size, absorption bands, saturation magnetization*

INTRODUCTION

After the introduction of theory of ferrimagnetism by Neel [1] in 1948, many researchers switch their work to study the properties of ferrites from micrometer to nanometer scale. Since from the last few years, several researchers have reported on the properties of pure and doped spinel ferrite nanoparticles because of their technological importance [2-7]. The advancement in electronic devices prepares them to work in the microwave frequency region with wider range such as mobile phones, LAN (wireless) systems, and bluetooth technologies. Growing use of microwave based equipments increases the electromagnetic pollution in this range creating a serious problem which has to be solved. To resolve the problem regarding electromagnetic pollution, development of handy electromagnetic radiation absorbers will be essential and demanding [8-9]. For the fabrication of electromagnetic radiation absorbers, ferrites [5], conducting fibers [10], ferromagnets [11], and carbon nano-tubes [12] are mostly used because of their high resistivity and very low eddy current losses. In particular cobalt ferrite attracted much interest due to its wide use in the fabrication of high density magneto-optical recording materials [13]. Cobalt ferrite nanoparticles with spinel structure show some interesting properties over the other materials such as very high saturation magnetization, high coercivity, large magnetocrystalline anisotropy, excellent chemical stability and good mechanical hardness. Cobalt ferrite shows inverse spinel structure and the percentage of inversion depends on the synthesis method and sintering conditions [14]. The intrinsic properties of ferrites can be controlled by synthesis conditions. Chemical methods of ferrite synthesis are the favorable routs in order to obtain the homogeneous powders with nano-particle size and desirable physical and chemical properties. In the present investigation we attempt to study the effect of sintering temperature on the structural and magnetic properties of $CoFeCrO_4$ ferrite nanoparticles synthesized by using sol-gel technique.

MATERIALS AND METHODS

Sample synthesis:

The synthesis method and synthesis condition plays an important role to decide the structural and magnetic behaviour of ferrites. Metal nitrates of constituent elements having chemical formula $Co(NO_3)_2.6H_2O$, $Fe(NO_3)_3.9H_2O$ and $Cr(NO_3)_3.9H_2O$ were used as starting materials and mixed in sufficient amount of double distilled water with their weight proportion in the composition. The whole mixture was placed on hot plate with magnetic stirrer. The mixture is stirred continuously with constant heating at 80^0C for 2-3 hours. Citric

acid was used as chelating agent in the ratio with metal nitrates as 1:3 and the pH of the mixture was maintained at 7 by adding liquid ammonia continuously. After continuous heating and stirring the density of the mixture increases and it converted into sol. After some time the puffy sol was converted into dried gel and suddenly auto ignited which in turns converted the mixture into burnt ash. The ash was grinded for homogenous mixture and then first heat treatment was given at 600^0C for 4 hours which produces almost the final product. These powders were divided into two equal parts, half is heated at 800^0C for 4 hours and remaining is heated at same temperature for 8 hours.

Characterization techniques:

Room temperature X-ray diffraction technique was employed to understand the crystal structure and phase formation. XRD patterns were recorded by using Cu-K_α radiations ($\lambda = 1.5406 \times 10^{-10}$ m) in the 2θ range of 20^0 to 80^0 with the scanning rate of 2 degree per min. the structural parameters such as lattice parameter (a), X-ray density (d_X), porosity (P) and average crystallite size were estimated by using X-ray diffraction data. Band positions and force constants at tetrahedral – A and octahedral –B sites were obtained by using Infrared spectra recorded in the frequency range of 300 cm^{-1} to 800 cm^{-1}. Morphological analysis of the samples was done by using scanning electron micrographs (SEM) and grain size of the samples was also estimated. Magnetic measurements were taken by using vibrating sample magnetometer (VSM) at room temperature.

RESULTS AND DISCUSSION

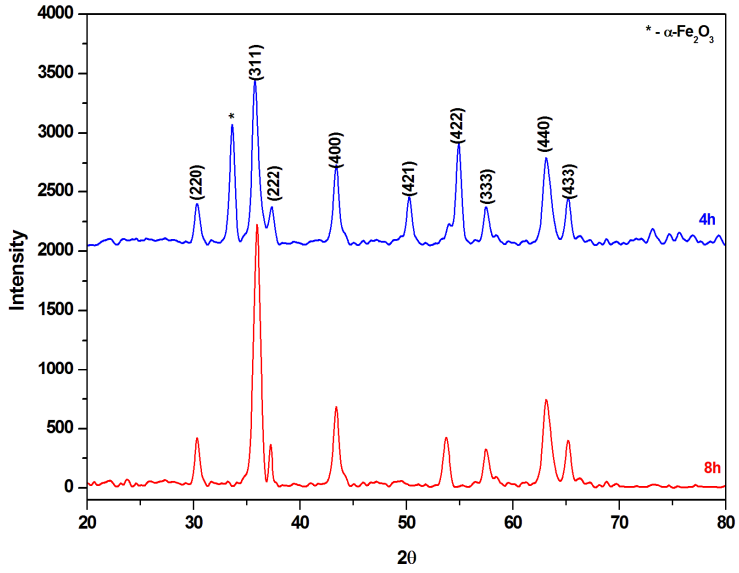

Fig. 1: XRD patterns of $CoFeCrO_4$ sintered at 800^0C for two different times.

Powder X-ray diffraction pattern shown in Fig. 1 shows sharp and intensive peaks indexed with the planes (220), (311), (222), (400), (422), (333), (440) and (433) which are corresponds to the standard crystal structure of the $CoFe_2O_4$ (JCPDS card No. 22-1086). An additional peak is observed for the sample heated for 4 hours which confirms the co-existence of α-Fe_2O_3. Secondary phase was disappears for the sample heated for 8 hours. It was observed that increasing the sintering time increases the phase purity of the samples. The sharp and broad Bragg'a lines confirm the formation of well defined crystalline samples.

Table 1: *Lattice constant (a), X-ray density (d_X), bulk density (d_B), percentage porosity (P), specific surface area (s), crystallite size (t), for $CoFeCrO_4$ samples.*

Time	**'a'** (Å)	**'V'** ($Å^3$)	**'d_X'** (gm/cc)	**'d_B'** (gm/cc)	**'P'** (%)	**'t' (nm)**	
						XRD	**SEM**
4h	8.321	576.2	5.320	4.039	31.72	15.13	45
8h	8.330	578.0	5.304	4.101	29.31	28.67	52

Lattice constant 'a' of $CoFeCrO_4$ was calculated by inserting the values of interplanner spacing's 'd' and miller indices in equation, $a = d\sqrt{N}$ [15] and the values are given in Table 1. It can be noticed that the lattice constant is affected by the sintering condition and it is increased with the increase in sintering time. Unit cell volume was calculated by using the average values of lattice constant and is given in Table 1 which shows the similar behaviour as of lattice constant. X-ray density of both the samples was calculated b using following relation,

$$d_x = \frac{nM}{N_A V} \qquad [1]$$

Where, n is number of molecules per unit cell (8 for cubic), M is molecular weight, N_A is Avogadro's number and V is unit cell volume. From Table 1, it is observed that X-ray density reduces from 5.320 gm/cc to 5.304 gm/cc as the sintering time increases from 4 hours to 8 hours. It is also observed that the bulk density 'd_B' calculated by using simple mass-volume relation increases as the sintering time increases. Calculated values of porosity are listed in Table 1, which shows decreasing trend with increasing time. This decrease in porosity is may be due to the decrease in bulk density and increase in crystallite size.

Broad XRD lines indicate the fine crystallites with nano-size. Most intensive peak (311) have been used to determine the crystallite size by using the following relation [16],

$$D_{XRD} = \frac{C\lambda}{B_{1/2}\cos\theta} \quad [2]$$

Where C is constant (shape factor = 0.9), λ is wavelength, $B_{1/2}$ is FWHM of (311) peak and θ is Bragg's angle. Estimated values of average crystallite size are given in Table 1. For the sample sintered for 4 hours, the crystallite size was obtained 15.13 nm and for the sample sintered for 8 hours it is 28.67 nm. Surface morphology of the samples was studied by using scanning electron micrographs shown in Fig. 2. The average grain size is obtained in the nanometer range and the results are in good agreement with the crystallite size obtained from the analysis of XRD data. For the samples sintered for 4 hours, average grain size is obtained 45 nm and it slightly increases for the samples sintered for 8 hours and is observed 52 nm. It is also observed that the samples are amorphous in nature and shows porous structure with some agglomerates particles. This agglomeration within the particles may be due to the high reactivity of the prepared samples with heat treatment and may also be come from the magneto-static interaction between the particles [17-19].

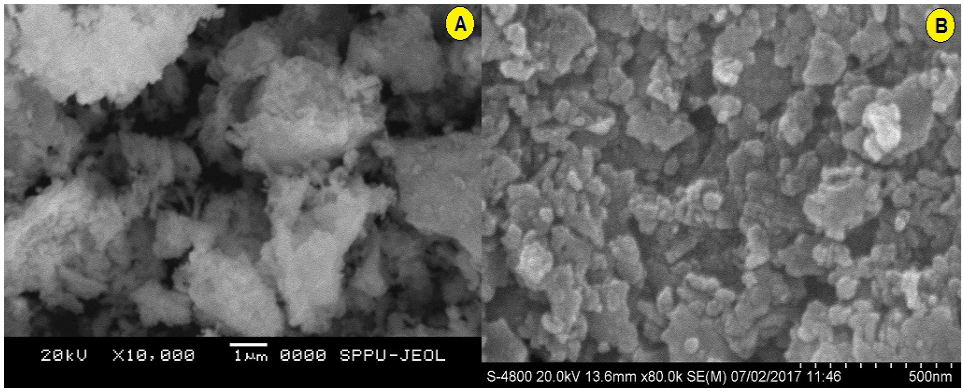

Fig. 2: SEM images of $CoCrFeO_4$ sintered for (A) 4h and (B) 8h.

Ion jump lengths (hopping lengths) of the samples are calculated by using the following relations [20],

$$L_A = \frac{a\sqrt{3}}{4} \quad [3]$$

$$L_B = \frac{a\sqrt{2}}{4} \quad [4]$$

Table 2 shows the calculated values of ion jump lengths and it can be seen that hopping lengths slightly increases with the increase in sintering temperature. This behaviour of hopping lengths is in accordance with the lattice parameter. The results are can also be explained on the basis of cation distribution over tetrahedral A-site and octahedral B-site.

Table 2: *Hopping lengths (L_A and L_B), absorption bands (ν_1 and ν_2), saturation magnetization (M_S), remnant magnetization (M_r), remnant ratio (M_r/M_s) and coercivity (H_C) for $CoFeCrO_4$ samples*

Time	'L$_A$' (Å)	'L$_B$' (Å^3)	Absorption bands		'M$_S$' (emu/gm)	'M$_r$' (emu/gm)	(M$_r$/M$_S$)	'H$_C$' (Oe)
			ν_1 (cm^{-1})	ν_1 (cm^{-1})				
4h	3.603	2.942	617.3	492.5	10.52	6.58	0.625	1471
8h	3.607	2.945	617.8	361.5	15.03	9.04	0.601	1132

Infrared spectra of all the samples recorded at room temperature in the range 300 cm^{-1} to 800 cm^{-1} are illustrated in Fig. 3 which shows two major absorption bands ν_1 and ν_2. The higher frequency band ν_1 is observed near 600 cm^{-1} while the lower absorption band ν_2 is observed near 400 cm^{-1}. For the sample sintered for 8 hours the higher frequency band slightly shifted towards lower frequency and the lower frequency band shifted towards lower frequency region. Values of band positions ν_1 and ν_2 are listed in Table 2. The difference in band positions is related to the stretching vibrations occurred between the metal cations and oxygen atoms due to the interactions at tetrahedral – A and octahedral – B sites [21].

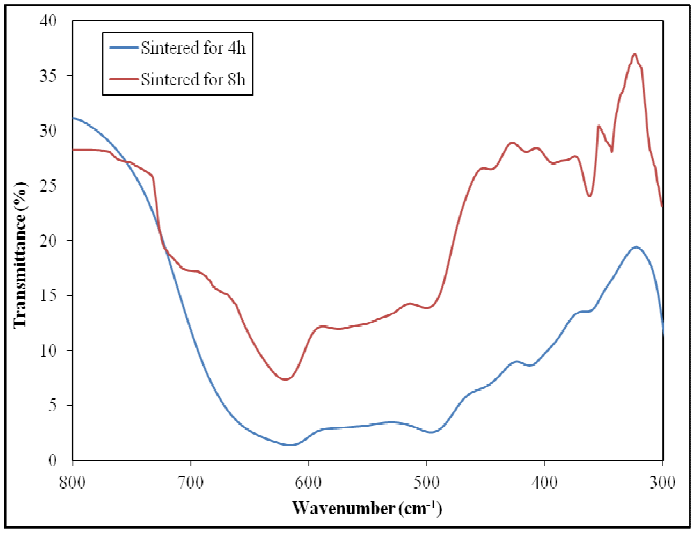

Fig. 3: Infrared spectra of $CoCrFeO_4$

Fig. 4 shows the magnetic hysteresis curves for $CoFeCrO_4$ sintered at 800^{0}C for at two different times 4h and 8h. The maximum field of 15kOe is applied for all the samples. The hysteresis loops exhibits a wide cycle and gives high saturation magnetization which is the indication of formation of hard ferrites. Increasing sintering time for Co-Fe-Cr ferrites increases the loop height and decreases the loop width.

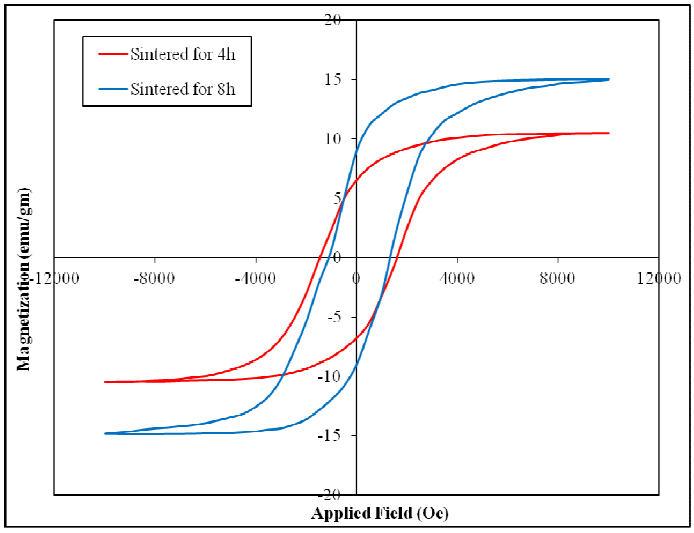

Fig. 4: Hysteresis loops of $CoCrFeO_4$

The values of saturation magnetization (M_S), coercivity (H_C) and remnant magnetization (M_r) obtained from the analysis of hysteresis loops are given in Table 2. Sintering conditions affects on the magnetic behaviour of the samples, and the saturation magnetization slightly increases with the increase in sintering time. Similarly the remnant magnetization varies from 6.58 emu/gm to 9.04 emu/gm.

Coercivity of the magnetic materials is closely related to the magneto-crystalline anisotropy and saturation magnetization by the following relation [22],

$$K = \frac{H_C M_S}{2} \qquad [5]$$

From equation 5 it can be seen that coercivity is inversely proportional to saturation magnetization and hence it shows opposite behaviour. For the samples sintered for 4 hours, coercivity is observed 1471 Oe and for the samples sintered for 8 hours it reduces to 1132 Oe. The variation in coercivity shows a size dependent behaviour which can be attributed to the combination of surface effect and surface anisotropy [23].

CONCLUSIONS:

Nanocrystalline powder of $CoCrFeO_4$ was successfully obtained by sol-gel technique. X-ray diffraction analysis confirms the cubic spinel structure of the samples. The sample sintered for 8 hours gives pure phase of the sample. Lattice parameter increases with the increase in sintering time. Grain size obtained from SEM images is observed in the nano-meter range which is in analogues with the results obtained from XRD analysis. Saturation magnetization increases and coercivity decreases with the increase in sintering time.

REFERENCES:

[1] L. Neel, *Ann. de Phys.*1948; 12:137

[2] M. V. Choudhari, S. E. Shirsath, A. B. Kadam, R. H. Kadam, S. B. Shelke, D. R. Mane; J. Alloys. Comp. 552 (2013) 443-450.

[3] S. E. Shirsath, R. H. Kadam, M. L. Mane, A. Ghesami, Y. Yasukawa, S. Liu, A. Morisako; J. Alloys. Comp. 575 (2013) 145-151

[4] J. H. Shim, S. Lee; *Phys. Rev. B* 2006; 73:064404.

[5] T. Tatrachuk, M. Myslin, I. Mironyuk, M. Bououdina, A. T. Pedziwiatr, R. Gargula, B. F. Bogacz, P. Kurzydlo; J. Alloys. Comp. 819 (2020) 152945.

[6] R. H. Kadam, A. R. Biradar, M. L. Mane, S. E. Shirsath; J. App. Phys. 112 (2012) 043902

[7] O. Suwalka, R. K. Sharma, V. Sebastian, N. Lakshmi, et. al. *J. Magn. Magn. Mater.* 2007; 313:198-203.

[8] M. R. Meshram, N. K. Agrawal, B. Sinha, P. S. Misra, *J. Magn. Magn. Mater.* 2004; 271:207.

[9] S. Sugimoto, S. Kondo, K. Okayama, D. Book, et. al. *IEEE Trans. Magn.* 1999; 35: 3154.

[10] Y. Nie, H. He, Z. Zhao, R. Gong, H. Yu, *J. Magn. Magn. Mater*. 2006; 306: 125.

[11] T. Kasagi, T. Tsutaoka, K. Hatakeyama, *Appl. Phys. Lett.* 2006; 88:172502.

[12] J. L. Xie, M. Han, L. Chen, R. Kuang et. al.; *J. Magn. Magn. Mater.* 2007; 314:37-42.

[13] B. H. Liu, J. Ding, *Appl. Phys. Lett.* 2006; 88:042506.

[14] I. H. Gul, A. Z. Abbasi,F. Amin, M. Anis-ur-Rehman, A. Maqsood; *J. Magn. Magn. Mater.*2007; 311:494-499.

[15] S. K. Gurav, S. E. Shirsath, R. H. Kadam, S. M. Patange et. al. *Mane; Mater. Res. Bull.*; 2013; 48: 3530-3536.

[16] S. E. Shirsath, R. H. Kadam, M. L. Mane, A. Ghesami et. al. *J. Alloys. Comp.* 2013; 575:145-151.

[17] C.A. Ross, *Rev. Mater. Res.* 2001; 31: 203.

[18] S.A. Majetich, M. Sachan, *J. Phys. D: Appl. Phys.* 2006; 39: R407.

[19] K. G. Kornev, D. Halverson, G. Korneva, Y. Gogotsi et. al. *Appl. Phys. Lett.* 2008; 92: 233117.

[20] B. Gillot, F. Jemmali; *Physica Status. Solidi (a);* 1983; 76:601.

[21] R. H. Kadam, Kirti Desai, V. S. Shinde, M. Hashim et. al. *J. Alloys. Comp.* 2016; 657: 487-494.

[22] K. S. Lohar, A. M. Pachpinde, M. M. Langade, R. H. Kadam et. al.; *J. Alloys Comp.* 2014; 604:204-210.

[23] S. E. Shirsath, R. H. Kadam, A. S. Gaikwad, Ali Ghasemi et. al.; *J. Magn. Magn. Mater.* 2011; 323:3104-3108